Published in final edited form as:

Circ Arrhythm Electrophysiol. 2019 July ; 12(7): e007294. doi:10.1161/CIRCEP.119.007294.

Plasticizer Interaction with the Heart: Chemicals Used in Plastic Medical Devices Can Interfere with Cardiac Electrophysiology

Rafael Jaimes III, PhD[1,2], **Damon McCullough, BS**[1,*], **Bryan Siegel, MD**[2,*], **Luther Swift, PhD**[1,2], **Daniel McInerney, BS**[1], **James Hiebert, BS**[1], **Erick A. Perez-Alday, PhD**[6], **Beatriz Trenor, PhD**[5], **Jiansong Sheng, PhD**[4], **F. Javier Saiz Rodriguez, PhD**[5], **Larisa G Tereshchenko, MD, PhD**[6], **Nikki Gillum Posnack, PhD**[1,2,3]

[1]Sheikh Zayed Institute for Pediatric Surgical Innovation

[2]Children's National Heart Institute, Children's National Health System

[3]Dept of Pediatrics, Dept of Pharmacology & Physiology, School of Medicine and Health Sciences: George Washington University, Washington DC

[4]CiPA Lab, LLC, Rockville, MD

[5]Universitat Politècnica de València, Valencia, Spain

[6]Knight Cardiovascular Institute, Oregon Health & Science University, Portland OR

Abstract

Background: Phthalates are employed as plasticizers in the manufacturing of flexible, plastic medical products. Patients can be subjected to high phthalate exposure through contact with plastic medical devices. We aimed to investigate the cardiac safety and biocompatibility of mono-2-ethylhexyl phthalate (MEHP), a phthalate with documented exposure in intensive care patients.

Methods: Optical mapping of transmembrane voltage and pacing studies were performed on isolated, Langendorff-perfused rat hearts to assess cardiac electrophysiology after MEHP exposure compared with controls. MEHP dose was chosen based on reported blood concentrations following an exchange transfusion procedure.

Results: 30-min exposure to MEHP increased the atrioventricular node (147 vs. 107msec) and ventricular (117 vs. 77.5msec) effective refractory periods, compared with controls. Optical mapping revealed prolonged action potential duration (APD) at slower pacing cycle lengths, akin to reverse use-dependence. The plateau phase of the APD restitution curve steepened and became monophasic in MEHP-exposed hearts (0.18 vs. 0.06 slope). APD lengthening occurred during late-phase repolarization resulting in triangulation (70.3 vs. 56.6 msec). MEHP-exposure also slowed epicardial conduction velocity (35 vs. 60 cm/sec), which may be partly explained by inhibition of $Na_v1.5$ (874 μM and 231 μM IC50, fast and late sodium current).

Correspondence: Nikki Gillum, Posnack, Ph.D., Sheikh Zayed Institute, 6th floor, M7708, 111 Michigan Avenue, NW, Washington, DC, 20010, Tel: (202) 476-2475, nposnack@childrensnational.org.

*contributed equally

Disclosures: None

Conclusions: This study highlights the impact of acute MEHP exposure, using a clinically-relevant dose, on cardiac electrophysiology in the intact heart. Heightened clinical exposure to plasticized medical products may have cardiac safety implications – given that action potential triangulation and electrical restitution modifications are a risk factor for early after depolarizations and cardiac arrhythmias.

Graphical Abstract

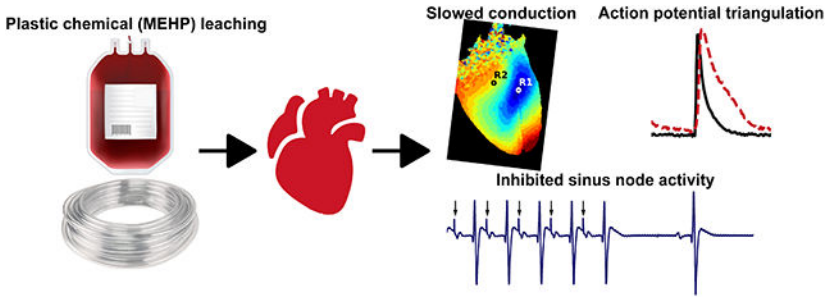

Keywords

electrophysiology; optical mapping; cardiotoxicity; cardiac tissue; phthalate; plasticizer; transmembrane voltage

Journal Subject Terms:

Electrophysiology; Physiology; Basic Science Research

Introduction

Plastics have revolutionized clinical care. Yet, despite the many advantages - concerns have been raised about the ubiquitous use of plastics in the clinical setting[1-3]. To manufacture flexible plastic products, phthalate esters are added to impart flexibility to otherwise stiff polyvinyl chloride (PVC) polymers. Di-2-ethylhexyl phthalate (DEHP) is the most commonly used plasticizer in FDA-approved medical devices, including blood storage bags, tubing circuits, enteral feeding tubes, endotracheal tubes and catheters[4]. In the finished product, DEHP can contribute up to 40% by weight in intravenous bags and 80% by weight in medical tubing. Since phthalate esters are hydrophobic and non-covalently bound to the PVC polymer, these additives are highly susceptible to leaching when in contact with blood, plasma, and other lipophilic solutions[5,6]. Consequently, heighted phthalate exposure has been observed in patients undergoing invasive medical procedures that employ large quantities of plastic materials – including cardiopulmonary bypass, extracorporeal membrane oxygenation, dialysis and transfusion procedures (see Table 1)[7-21]. As an example, a neonatal exchange transfusion procedure resulted in plasma concentrations as high as 38 μM DEHP and 54 μM MEHP (mono-2-ethylhexyl phthalate), the primary metabolite of DEHP[13]. Whereas multiple medical procedures can increase a patient's cumulative phthalate exposure to levels that are 4,000 – 160,000 times higher than deemed safe[7]. Importantly, phthalate levels can remain elevated in the blood for hours (e.g., blood

transfusion; 5-24 hour half-lives)[22,23] to weeks (e.g., ECMO support, ICU patient) depending on the course of treatment[19].

Incidental plastic chemical exposure during medical procedures is virtually unavoidable, yet the direct impact on patient health remains unclear. Since phthalates structurally resemble natural hormones, they can exert endocrine-disrupting properties and interfere with an array of biological processes[7,24,25]. Moreover, these low-molecular weight chemicals have been shown to interact with ion channels, nuclear receptors, and other cellular targets. Accordingly, phthalates are likely to have a global impact on human health that is multifactorial. Indeed, epidemiological studies have reported associations between phthalate exposure and a broad range of health conditions, including metabolic disturbances, reproductive disorders, inflammatory conditions, neurological disorders and cardiovascular disease[24-31]. The latter is particularly worrisome – since patients who are most susceptible to hospital-based phthalate exposures are often at heightened risk for cardiovascular complications, including those undergoing multiple transfusions, chronic transfusions (sickle cell, thalassemia) and/or support procedures (extracorporeal membrane oxygenation, cardiopulmonary bypass, dialysis)[4,9,19,32-34]. Local and systemic reactions to plastic chemicals may add an extra ‘insult’ to patients who are prone to secondary complications, including: hypoxia (congenital heart defect patients), ischemia-reperfusion injury (cardiac surgery patients), post-operative arrhythmias, cardiac iron overload, pulmonary hypertension, impaired contractility and diastolic dysfunction.

Indeed, animal studies have shown a causal relationship between phthalate exposure and subsequent alterations in cardiovascular function[35-39]. Using a rodent heart-lung preparation, Labow, et al. showed that phthalates exert a hypertensive effect on the pulmonary vasculature[38]. This group also showed that phthalate exposure has a negative inotropic effect on isolated human atrial trabeculae, thus highlighting the applicability to humans[36]. Our group has also shown that phthalate exposure alters calcium handling and contractility *in vitro*, using rodent and human cardiomyocytes[40,41]. Moreover, phthalate exposure was shown to reduce gap junctional connexin-43[40,41]– which decreased intercellular coupling and slowed conduction velocity. Therefore, we hypothesized that phthalate exposure may directly impact cardiac electrophysiology in an intact heart.

To test this hypothesis, we comprehensively assessed the electrophysiological effects of mono-2-ethylhexyl phthalate (MEHP) using isolated, intact rodent hearts. Cardiac electrophysiology parameters were measured at baseline, and again after treatment with either control or MEHP-supplemented media perfusion (30 min). To address clinical relevance, the MEHP dose (60 μM) selected for heart perfusion was comparable to patient exposure following an exchange transfusion procedure[42] and/or measured levels in stored blood products[4,43].

Methods

The authors declare that data that supports the findings of this study are available within the article.

Isolated heart preparation

Animal protocols were approved by the Institutional Animal Care and Use Committee of the Children's Research Institute, and followed the National Institutes of Health's *Guide for the Care and Use of Laboratory Animals*. Experiments were conducted using adult, male Sprague-Dawley rats (>8 weeks old, >280 g, Taconic Biosciences). Animals were housed in conventional rat cages in the Research Animal Facility under standard environmental conditions (12:12 hour light:dark cycle, 64 – 78C, 30-70% humidity, free access to reverse osmosis water, corn cob bedding and food (2918 rodent chow, Envigo)). Animals were anesthetized with 3-5% isoflurane, the heart was excised and then transferred to a temperature-controlled (37°C) constant-pressure (70 mmHg) Langendorff perfusion system for electrophysiology and optical mapping experiments. Excised hearts were perfused with Krebs-Henseleit buffer bubbled with carbogen throughout the duration of the experiment, as previously described (~1 hour)[44].

General protocol

Mono(2-ethylhexyl) phthalate (MEHP, 93+%, Wako Chemicals) stock solution was prepared in 99+% dimethyl sulfoxide (DMSO), and the working concentration was prepared directly in perfusate media with a total DMSO concentration of <0.001%. To avoid a bolus exposure, the perfusion system was designed to premix MEHP with perfusate media to a desired concentration before entering the aorta. Cardiac electrophysiology was assessed under baseline conditions (control media perfusion) and again after either control media perfusion or 60 μM MEHP-supplemented media perfusion (30 min). This allowed us to control for electrophysiology changes that could be attributed to procedure (control baseline vs control 30-min), individual animal differences, and MEHP-treatment (control 30-min vs MEHP 30-min). For clinical relevance, the MEHP dose (60 μM) was selected based on an upper clinically relevant exposure following an exchange transfusion procedure[42], and within the range of measured levels in stored blood products [4,43].

Electrophysiology measurements

A reference electrode was positioned proximal to the right atrium (RA) and a measuring electrode proximal to the apex to acquire a pseudo-electrocardiogram in the lead II configuration (differential amplifier with 1000x gain). During sinus rhythm, ECG signals were collected to analyze heart rate, beat rate variability, atrioventricular conduction (PR interval) depolarization time and repolarization time (RJ_{point}, RT)[45]. Signals were acquired in iox2 (emka Technologies), and ECG segments were computed in ecgAUTO (emka Technologies).

For determination of atrioventricular (AV) nodal effective refractive period (AVNERP), Wenckebach cycle length (WBCL) and sinus node recovery time (SNRT), a coaxial stimulation electrode (Harvard Apparatus, Holliston, MA) was placed on the RA. AVNERP was defined as the maximum extrastimulus interval (S1-S2) during atrial pacing that failed to conduct through the AV node, as indicated by loss of ventricular capture. WBCL was defined as the maximum pacing cycle length (PCL) during atrial pacing that caused the Wenckebach phenomenon. SNRT was measured to assess the automaticity of the sinoatrial node, and defined as the time delay between the last paced atrial depolarization and the first

sinus beat (5 sec electrical stimulation at 200 msec PCL). A stimulator (Bloom Electrophysiology, Denver, CO) was set to 1 msec pulse width at 1.5x diastolic current threshold. For ventricular pacing, a 0.25 mm diameter tungsten, unipolar, cathodal electrode was placed on the LV epicardium and centered in the imaging field. A stainless steel indifferent electrode was placed under the heart. To determine the ventricular effective refractory period (VERP) within 10 msec, dynamic pacing (S1-S1) was performed during optical mapping. An arrhythmia score was designated for each individual heart after the dynamic pacing protocol, wherein the most severe electrical disturbance was classified (1 = single premature ventricular contraction (PVC), 2 = bigeminy/salvos, 3 = ventricular tachycardia or fibrillation)[46].

Ventricular conduction frequency composition assessment

High resolution (2000Hz) unfiltered digital pseudo-ECG recordings were analyzed using a custom MATLAB (MathWorks, Inc., Natick, MA) software application. Normal sinus median beat was constructed out of 436 normal sinus beats, as previously described [47]. Appropriate selection of beats was confirmed by investigator (EAPA) with the aid of a graphical display. From the median beat obtained, QRS was measured from QRS onset to J-point[48]. The power spectral density (PSD) was measured on the median beat of the ECG signal[49] using a non-parametric Fast-Fourier transform algorithm based on the Welch-Bartlett power estimation method[50], with a Hanning window of length eight samples and a 50% overlap between segments. From the Nyquist frequency, the available frequency range was from 0 to 1000Hz, however, the frequency composition was calculated on five subsets of 100Hz frequency intervals from 0Hz to 500Hz. The relative contribution of frequencies was normalized over the total power.

Optical mapping

After establishing a baseline heart rate (10 min), the perfusate was supplemented with 10 μM (−/−) blebbistatin (Sigma-Aldrich) to reduce motion artifact for imaging experiments[51]. The heart was loaded with a potentiometric dye (62.1 μg RH237, 1 minute staining) through a bubble trap located proximal to the aortic cannula[52,53]. The epicardium was illuminated with two broad LED spotlights (530 nm, 200 mW, Mightex). RH237 fluorescence was longpass filtered (680+ nm, Chroma Technologies) and optical action potentials were acquired using a fixed focal lens (17mm, f/0.95, Schneider Optics) attached to a sCMOS camera (Zyla 4.2 PLUS, Andor Technology). The camera sensor was cropped to 384×256 pixels and set to an exposure time of 1.219 ms resulting in the acquisition of 16-bit monochrome images at 814 frames per second for two seconds. Optical maps were acquired during each PCL (S1-S1; 250 – 80 msec, 10 msec increments). A custom MATLAB (MathWorks, Natick, MA) script was used to calculate the action potential durations (APD) to percent repolarization (APD30, 80, 90) for every beat in the recording, as previously described. APD triangulation was defined as the difference between APD90 and APD30[54]. Restitution curves were generated by plotting APD80 against PCL; curves were then analyzed as either monophasic or biphasic (where applicable) to determine slopes as indicated by Franz[55]. APD alternans were defined as sequential APD80 measurements that differed by >4msec.

Image and signal processing

Data analysis was performed using a custom MATLAB script. A region of interest (<20 pixel radius) was selected from the raw image, averaged, and plotted against time. Drift removal was performed by subtraction of a polynomial fit if necessary. To remove high frequency noise, a 5th order Butterworth low-pass filter was applied to the resulting signals with a cut-off frequency adjusted between 50-150 Hz. A peak detector was then used to measure the total number of action potentials in the file across time. Characteristics from each event are measured and averaged, including APD30, APD80 and APD90, as described previously. Image processing was performed and isochrone activation maps were constructed in *RHYTHM*[56]. The background was removed, convolved with a 15×15 uniform kernel for box blurring and then time signals were low-pass filtered below 100 Hz. The activation time of every pixel on the heart was defined as the maximum derivative of the action potential or transient upstroke. To measure epicardial conduction velocity, activation maps were subsequently loaded into *ORCA*[57] and measured at a minimum of 18 angles separated by 10 degrees each from the pacing stimulus with the median conduction velocity reported. Subsequent electrical wave propagation images were then constructed using custom Python scripts and plotted with matplotlib[58].

Whole-cell voltage-clamp recordings

Recordings were performed at room temperature (22-25°C) using HEK-293 cells stably transfected with Nav1.5 cDNA. For Nav1.5 recordings, the extracellular solution (mM) included: 137 NaCl, 10 HEPES, 4 KCl, 1 MgCl2, 1 CaCl2, 10 dextrose, and the intracellular solution included: 120 Aspartic Acid, 120 CsOH, 10 CsCl, 10 HEPES, 10 EGTA, 5 MgATP, 0.4 TrisGTP. The voltage protocol (1 sec duration) was repeated at 0.1Hz. Briefly, cells were repolarized from −95 mV to −120 mV for 200 ms, then depolarized from −120 mV to −15 mV for 40 ms and further depolarized to +40 mV for 200 ms, followed by a voltage ‘ramp down’ phase for 100 ms from +40 mV to −95 mV. Nav1.5 late current was induced by 20 nM anemone toxin (ATX-II) in the extracellular solution, which allowed for the study of late sodium current contribution from Nav1.5 that is separate from fast sodium current, as previously described[59]. Nav1.5 fast current was measured in the absence of ATX-II. For positive control, 30 μM TTX (tetrodotoxin, sodium channel blocker) was directly applied to recordings and resulted in 98.3±0.7% Nav1.5 current block (n=3). To ensure baseline recording was stable enough for drug application, cells were presented with this voltage protocol in control solution until Nav1.5 current amplitudes for 12 consecutively recorded current traces (2-min duration) exhibit <10% difference. Effects were monitored for 3 minutes before and after application of MEHP (n=4 per dose). To quantify drug potency against Nav1.5 channels, the steady state Nav1.5 current amplitude (averaged value from 5 steady state current traces) in drug solution were divided by the averaged amplitude from the last 5 traces measured in control solution to calculate the fractional block. Then fractional block was plotted against drug concentration tested, fitted with the Hill Equation to generate an IC50 and the Hill coefficient.

In silico modeling

Human ventricular action potentials were simulated using previous established models and conductance [60,61]. The block of fast and late sodium, I_{Na} and I_{NaL}, respectively, were provoked with the computed IC50 from MEHP determined by whole-cell recordings (see previous section) as previously described[62]. The isolated epicardial cellular model was paced with 1000 pulses (−80 μA/μF, 0.5 msec) at PCL=250 msec in the presence of 60 μM MEHP.

Statistical Analysis

Statistical analysis was performed using the R software package and Stata MP 15.1 (StataCorp, College Station, TX). Data normality was confirmed by Shapiro-Wilk test. Datasets were compared using a two-sample Student's independent T-test between the two treatment groups (30-min control, 30-min MEHP treated) or paired T-test between baseline and 30-min timepoints. Significance was defined as $p \leq 0.05$. Results were reported as mean ± standard error mean, from a minimum of 5 animals per group as indicated. As distribution of PSD variables was skewed, we used Wilcoxon rank-sum test to compare groups (control vs. MEHP-treated). Wilcoxon matched-pairs signed-ranks test was used for paired comparison of PSD changes before and after MEHP treatment. Variables with skewed distribution are presented as median and interquartile range (IQR). Arrhythmia incidence was compared using the Chi-square test.

Results

Effects of MEHP exposure on cardiac automaticity and beat rate variability during sinus rhythm

ECG characteristics were quantified at two time points – first under baseline conditions, and again after 30 minutes of control or 60 μM MEHP-supplemented media perfusion during sinus rhythm (Figure 1A). Example ECG traces are shown in Figure 1B. Heart rate at 30 minutes was comparable between experimental groups, 172 BPM in control and 178 BPM in MEHP-treated hearts (Figure 1C, D). Beat rate variability was assessed as a cumulative index of automaticity and sinus node discharge. Although both root means successive square difference (rMSSD) and standard deviation of the normal RR intervals (SDNN) trended higher in MEHP-treated hearts (9.4 ± 2.4 msec and 17.3 ± 4.2 msec, respectively) compared with controls (5.4 ± 1.7 msec and 11.9 ± 2.5 msec, respectively), neither parameter was significant (rMSSD p=0.19, SDNN p=0.28), Figures 1E and F. MEHP-treatment increased RJ_{point} and RT intervals by 55% and 30%, respectively (Figure 2), both readily identifiable indicators of depolarization and repolarization in the excised rodent heart[45] (Figures 1G, H). Atrioventricular (AV) conduction delay was also measured during sinus rhythm. AV conduction remained relatively stable in control hearts, as indicated by a PR interval time of 43 ± 2 msec at baseline and 47 ± 2 msec after 30-min perfusion. In comparison, the PR interval time increased by 44% in MEHP-treated hearts (41 ± 1 msec baseline, 59 ± 3 msec, $p < 0.05$), Figure 1I)

Electrophysiological Study

Sinus node function was further investigated by measuring sinus node recovery time (SNRT), which was delayed by 54% in MEHP-treated hearts (532 ± 57 msec) compared with control hearts (345 ± 10 msec, p=0.01, Figure 2A-C). Wenckebach cycle length (WBCL) trended longer in MEHP-treated hearts compared with controls, 155.8 ± 12.4 to 126.6 ± 4.5 (p=0.07, Figure 2D). AV node conduction refractoriness was interrogated by implementing an atrial pacing protocol to measure AVNERP, which was significantly longer in MEHP-treated hearts compared with controls, 147 ± 13 msec to 107 ± 4.4 ms ($p<0.05$, Figure 2E). These results suggest that MEHP may directly increase AV nodal refractoriness.

Effects of MEHP exposure on ventricular conduction and refractoriness during sinus rhythm

ECG frequency content was also analyzed during sinus rhythm, as high frequencies during depolarization are associated with abnormal or slowed conduction[48,63]. In MEHP-treated hearts, contribution of high frequencies (400-500Hz) was increased by 0.032% (IQR: −0.008 to 0.20%), whereas in control group, contribution of the same frequency band (400-500Hz) decreased by 0.06% (IQR: 0.04 to 1.19%), p=0.076. ECG lead placement among isolated hearts proved difficult due to the lack of anatomical markers and consistency in positioning of the heart relative to ECG leads, making experimental variability between individual hearts high for power spectral density measurements. Follow-up studies were performed using optical mapping, since APD and VERP measurements may more accurately predict alterations in ventricular repolarization in the rodent heart[64].

Effects of MEHP exposure on epicardial conduction and refractoriness during epicardial pacing

Optical mapping of transmembrane voltage signals was performed to evaluate action potential shape and duration, using an epicardial pacing protocol. APD at 80% repolarization (APD80) was assessed until VERP was reached, and APD80 values were compared between the timed control and MEHP-treatment group giving rise to the electrical restitution curves (Figure 3A). Ventricular refractoriness was determined during our optical mapping protocol which involves ventricular pacing at both baseline and 30-min conditions. VERP was 51% longer in MEHP-treated hearts (117 ± 9.5 msec) compared with time-matched controls (77.5 ± 5.5 msec, $p<0.05$ Figure 3B). A longer refractory period suggests that MEHP exposure slows repolarization. MEHP-treated hearts displayed a monophasic restitution curve with a slope of 0.18 throughout (steep portion only, no plateau), as compared to controls which displayed a biphasic shape (steep and plateau phases). The steep slope of the controls was like that of the MEHP-group at 0.17, and the slope of the plateau phase was 0.06. Importantly, monophasic restitution curves are associated with an increased risk of electrical alternans[55,65]. With a lengthened VERP in MEHP-treated hearts, loss of capture at PCLs <100 msec limited APD measurements in the MEHP group.

APD30 and APD90 were measured to compute the triangulation of the action potential. At a selected fast PCL (140 msec), there were no significant differences between control and MEHP (Figure 3C). APD30 prolonged with time in both groups (Figure 3D), with no difference between APD90 and AP triangulation (Figures 3E and 3F, respectively). At a

slower PCL (240 msec), APD90 was significantly prolonged in MEHP-treated hearts (93.5 ± 3.5 msec) compared with controls (75.2 ± 4.2 msec, p=0.02) (Figure 3G). The lengthening of APD90 (Figure 3I) without a significant change in APD30 (Figure 3H) led to an increase in the AP triangulation (APD90-APD30)[54]; AP triangulation was 56.6 ± 4.5 msec in the controls and increased to 70.3 ± 2.9 msec in the MEHP group (Figure 3J). These results suggest that MEHP exposure exerts a reverse use-dependence effect, wherein myocyte refractoriness and action potential prolongation is increased at slower heart rates[66].

Electrical alternans and arrhythmia susceptibility

AP triangulation, reverse use-dependence and a monophasic electrical restitution curve with no plateau phase have been associated with an increased propensity for electrical alternans and arrhythmias[54,55,67]. APD instability was assessed by quantifying the incidence of electrical alternans, or sequential beat-to-beat variations in APD such as displayed in Figure 4A. The threshold of electrical alternans was observed in MEHP-treated hearts at a cycle length of 122 ± 11 msec, compared to 96 ± 6 msec PCL (p=0.06, Figure 4B). Rodent hearts are resistant to fibrillation, due in part to the small tissue mass[45]. Therefore, to assess arrhythmia susceptibility, each individual heart was scored by the most severe electrical disturbance encountered during the electrophysiology study at the end of the experiment. Arrhythmia incidence was significantly increased in MEHP-treated hearts, compared with controls ($p<0.05$, Figure 4C).

MEHP exposure slows conduction velocity

Our previous *in vitro* studies suggest that phthalate esters uncouple neighboring cardiomyocytes, resulting in slowed conduction and an arrhythmogenic phenotype[40]. To test whether this effect was observed in an intact heart, conduction velocity (CV) across the epicardial surface was measured using optical mapping and a unipolar, cathodal pacing electrode. The electrode was centered in the field of view and 10-degree increments were used to measure ≥180 degrees of coverage for longitudinal and transverse CV measurements. Optical mapping confirmed that paced beats propagated as elliptical wavefronts that emanated from the pacing electrode (Figures 5A-D). For depiction, we show two selected regions for each heart across the epicardial surface and the conduction time from pacing intiation to the distal site under control (Figure 5E) and MEHP (Figure 5F) conditions. To investigate CV restitution, both a slow (240 msec) and fast (140 msec) PCL were selected for CV measurements. Incidentally, CV increased slightly between baseline and 30-min timed recordings in control hearts at both pacing rates (Figures 5G and H). However, MEHP-treated hearts displayed 47% slower CV at 240 msec PCL (Figure 5G) and 42% slower CV at 140 msec PCL (Figure 5H) compared with time-matched controls.

MEHP inhibits sodium channel current

Slowed myocardial conduction velocity can be attributed to a reduction in sodium channel current, anatomical obstacles and/or diminished cellular coupling (e.g., gap junctions). Since the latter two mechanisms may take additional time (exceeding 30-min chemical exposure), we focused our attention on the direct effects of MEHP on sodium current. The onset of current suppression was concentration-dependent (Figure 5I). MEHP suppressed fast and late sodium current (I_{Na}) with a half-maximal inhibitory concentration (IC50) of 874 μM

and 231 μM, respectively. TTX (30 μM), a potent neurotoxin that blocks Nav1.5, served as a positive control resulting in >96% inhibition for all experiments (data not shown). Using *in silico* modeling combined with IC50 values, 60 μM MEHP is expected to decrease dV/dt by 4.6% (215 to 205 mV/ms), based on a human epicardial action potential at BCL = 250msec.

Discussion

This study is the first to examine the impact of MEHP on the electrophysiology of the intact heart, using a clinically-relevant concentration that was comparable to patient exposure following an exchange transfusion procedure[42] and/or measured levels in stored blood products[4,43]. Importantly, we show that acute MEHP exposure results in slowed atrioventricular conduction, slowed epicardial conduction velocity, and increased atrioventricular & ventricular refractory periods. Optical mapping studies revealed a prolonged action potential duration at slower pacing cycle lengths, akin to reverse use-dependence. MEHP-treated hearts also displayed a triangulated action potential and a steeper electrical restitution curve – both of which have been associated with an increased propensity for electrical alternans and arrhythmias.

Automaticity and sinus node function

Automaticity in the isolated heart is determined by a balance between inward and outward currents ('voltage clock')[68-70] and calcium oscillations ('calcium clock')[71], and as such, alterations in the spontaneous beating rate can serve as a cumulative index of cardiac excitability. Previous studies have reported bradycardia following phthalate exposure *in vivo*[39] (>20 mg/kg MEHP), *in vitro*[72] (10 μM DEHP), and using an isolated heart model[73] (250 μM DEHP). In the current study, we observed comparable heart rates between treatment groups (control, MEHP) at the dose and duration chosen for the study (60 μM MEHP, 30 min). Alterations in automaticity may become more pronounced after longer treatment times, with higher concentrations, and/or exposure to the parent compound vs metabolite (DEHP vs MEHP). We also examined beat rate variability as a cumulative index of automaticity and sinus node discharge. Both rMSSD and SDNN trended higher in MEHP-treated hearts, but neither parameter was statistically significant. Sinus node function was directly measured using a pacing protocol to quantify SNRT, which was significantly delayed by 54% in MEHP-treated hearts. These results suggest an underlying effect of phthalate esters on potassium channel current and/or calcium handling in the sinoatrial node[74]; indeed, alterations in calcium cycling and contractility have been reported in cardiac preparations treated with phthalate esters[36,41].

Atrioventricular conduction

We assessed the direct effect of MEHP exposure on intrinsic atrioventricular electrical conduction, by quantifying PR interval, AVNERP and WBCL. Similar to a previous report by Aronson, et al.[73], we observed a 44% prolongation of PR interval time in MEHP-treated hearts compared with controls – concomitant with a 37% increase in AVNERP and 23% increase in WBCL. Negative dromotropy through the AV node is commonly observed with cholinergics – and at least one study has shown that the effects of phthalate esters on human atrial trabeculae are partially inhibited by atropine, suggesting an interaction with

cholinergic receptors[36]. Alternatively, an interaction between phthalate esters and potassium and/or calcium channels could also alter nodal conduction. Indeed, a recent whole-cell patch clamp study demonstrated that phthalate exposure (10-100 μM DEHP, parent compound of MEHP) blocks L-type calcium channels in vascular smooth muscle cells[75].

Ventricular conduction and electrical instability

Using an isolated intact heart preparation, we observed significant effects on ventricular conduction and repolarization. During sinus rhythm, MEHP-treatment prolonged RJ_{point} and RT intervals, indicating a slowing of the internal conduction system. Notably, recent studies have highlighted the utility of APD and VERP measurements as precise indicators of ventricular repolarization[64]. Using an epicardial pacing protocol, we observed a 51% increase in VERP and 24% increase in APD90 time at slower PCL. On the surface, this result might suggest a beneficial, anti-arrhythmic effect of acute MEHP exposure. Though importantly, APD prolongation is a key contributor to electrical instability when the AP is triangulated[54,67] – as is the case with pharmaceuticals that exert off-target Ikr/hERG interactions that can set the stage for EADs and Torsades[76]. Moreover, reverse-use dependence can also be pro-arrhythmic as the APD restitution slope changes shape and becomes steeper. Similar to the effects of sotolol on electrical restitution[77], we observed significant APD90 prolongation at slower PCL (>190 msec) and a steep, monophasic APD restitution curve in MEHP-treated hearts. A steeper APD restitution slope with lack of plateau phase at longer basic cycle lengths can lead to an increased spatial dispersion of restitution properties, therefore creating a pro-arrhythmic milieu and electrical alternans[65]. Due to a significant difference in VERP, we were unable to reach faster pacing rates in MEHP-treated hearts; but, electrical alternans were observed at longer PCL in MEHP hearts (122 msec) compared with controls (96 msec). We also observed a 42-47% decrease in epicardial conduction velocity, which can be partly attributed to an immediate inhibitory effect of MEHP on sodium channels. Indeed, fast and late sodium channel current was inhibited by MEHP (IC50 874 μM and 231 μM MEHP, respectively) using an HEK293 cell line stably expressing $Na_v1.5$. IC50 values were subsequently used for human *in silico* modeling, predicting a modest slowing of dV/dt. Though the latter was more modest than anticipated, additional voltage clamp studies using a cardiomyocyte model may aid in the interpretation of these results.

Due to the acute nature of the observed effects of MEHP exposure, our study suggests that phthalate esters interfere with ionic currents in the myocardium – and these effects may be multifactorial. Unfortunately, the rodent myocardium is not ideal for assessing arrhythmia incidence due to its small size and robustness to fibrillation[45]. Future electrophysiological studies are needed, in a larger animal model, to definitively draw a conclusion on the arrhythmogenic potential of MEHP and other phthalate esters. Clinical studies showed that abnormal slow conduction in patients with ventricular arrhythmias can manifest by increased power of high frequencies within the ECG signal [63,78]. In this study, we observed a trend towards higher contribution of high frequencies within QRS– but, power spectral density measurements proved difficult due to variability in excised heart positioning relative to ECG lead placement.

Study limitations

The scope of the study was limited to the effect of acute (30 min) MEHP exposure on cardiac electrophysiology, using an isolated heart model. Such a model prevents the investigation of longer exposure time, and *ex vivo* results may differ from *in vivo* studies with an intact vascular and autonomic nervous system. The reported results are also limited to the effect of MEHP, and therefore, do not account for additional effects that may be caused by DEHP (the parent compound) or other secondary metabolites. The presented study was also limited to a single dose of MEHP, which was chosen based on the reported blood concentration following an exchange transfusion procedure.

Conclusion

This study reports the electrophysiological effects of mono-2-ethyhexyl phthalate on intact, isolated rodent hearts. The increase in action potential triangulation and altered action potential duration restitution curve are both indicators of increased arrhythmic risk.

Acknowledgments:

The authors gratefully acknowledge Manelle Ramadan, BS, Morgan Burke, BS, and Ashish Doshi, MD, PhD for technical assistance.

Sources of Funding: This work was supported by the National Institutes of Health (R00ES023477 and R01HL139472 to N.G.P), Children's Research Institute and Children's National Heart Institute. We thank the generosity of the NVIDIA corporation for the graphics processing unit to perform CUDA-enabled image processing.

References:

1. Braun JM, Sathyanarayana S, Hauser R. Phthalate exposure and children's health. Curr Opin Pediatr. 2013;25:247–254. [PubMed: 23429708]
2. Luban N, Rais-Bahrami K, Short B. I want to say one word to you--just one word--"plastics". Transfusion. 2006;46:503–506. [PubMed: 16584424]
3. van der Meer PF, Reesink HW, Panzer S, Wong J, Ismay S, Keller A, Pink J, Buchta C, Compernolle V, Wendel S, Biagini S, Scuracchio P, Thibault L, Germain M, Georgsen J, Bégué S, Dernis D, Raspollini E, Villa S, Rebulla P, Takanashi M, de Korte D, Lozano M, Cid J, Gulliksson H, Cardigan R, Tooke C, Fung MK, Luban NLC, Vassallo R, Benjamin R. Should DEHP be eliminated in blood bags? Vox Sang. 2014;106:176–195. [PubMed: 24330039]
4. FDA. Safety Assessment of Di(2-ethylhexyl)phthalate (DEHP) Released from PVC Medical Devices. [Internet]. 2002;https://no Available from: https://noharm-uscanada.org/sites/default/files/documents-files/116/Safety_Assessment_of_DEHP.pdf
5. Loff S, Kabs F, Witt K, Sartoris J, Mandl B, Niessen KH, Waag KL. Polyvinylchloride infusion lines expose infants to large amounts of toxic plasticizers. J Pediatr Surg. 2000;35:1775–1781. [PubMed: 11101735]
6. Rais-Bahrami K, Nunez S, Revenis ME, Luban LC, Short BL. Adolescents exposed to DEHP in plastic tubing as neonates: research briefs. Pediatr Nurs. 2004;30:406, 433. [PubMed: 15587534]
7. Mallow EB, Fox MA. Phthalates and critically ill neonates: device-related exposures and non-endocrine toxic risks. J Perinatol. 2014;34:892–897. [PubMed: 25357096]
8. Sjöberg P, Bondesson U, Sedin G, Gustafsson J. Dispositions of di- and mono-(2-ethylhexyl) phthalate in newborn infants subjected to exchange transfusions. Eur J Clin Invest. 1985;15:430–6. [PubMed: 3938415]
9. Barry YA, Labow RS, Keon WJ, Tocchi M, Rock G. Perioperative exposure to plasticizers in patients undergoing cardiopulmonary bypass. J Thorac Cardiovasc Surg. 1989;97:900–905. [PubMed: 2657224]

10. Peck CC, Odom DG, Friedman HI, Albro PW, Hass JR, Brady JT, Jess DA. Di-2-ethylhexyl phthalate (DEHP) and mono-2-ethylexyl phthalate (MEHP) accumulation in whole blood and red cell concentrates. Transfusion. 1979;19:137–146. [PubMed: 432924]
11. Pollack GM, Buchanan JF, Slaughter RL, Kohli RK, Shen DD. Circulating concentrations of di(2-ethylhexyl) phthalate and its de-esterified phthalic acid products following plasticizer exposure in patients receiving hemodialysis. Toxicol Appl Pharmacol. 1985;79:257–267. [PubMed: 4002227]
12. Faouzi MA, Dine T, Gressier B, Kambia K, Luyckx M, Pagniez D, Brunet C, Cazin M, Belabed A, Cazin JC. Exposure of hemodialysis patients to di-2-ethylhexyl phthalate. Int J Pharm. 1999;180:113–121. [PubMed: 10089298]
13. Sjoberg PO, Bondesson UG, Sedin EG, Gustafsson JP. Exposure of newborn infants to plasticizers. Plasma levels of di-(2-ethylhexyl) phthalate and mono-(2-ethylhexyl) phthalate during exchange transfusion. Transfusion. 1985;25:424–428. [PubMed: 4049487]
14. Shneider B, Schena J, Truog R, Jacobson M, Kevy S. Exposure to di(2-ethylhexyl)phthalate in infants receiving extracorporeal membrane oxygenation. N Engl J Med. 1989;320:1563.
15. Karle VA, Short BL, Martin GR, Bulas DI, Getson PR, Luban NL, O'Brien AM, Rubin RJ. Extracorporeal membrane oxygenation exposes infants to the plasticizer, di(2-ethylhexyl)phthalate. Crit Care Med. 1997;25:696–703. [PubMed: 9142038]
16. Plonait SL, Nau H, Maier RF, Wittfoht W, Obladen M. Exposure of newborn infants to di-(2-ethylhexyl)-phthalate and 2-ethylhexanoic acid following exchange transfusion with polyvinylchloride catheters. Transfusion. 1993;33:598–605. [PubMed: 8333024]
17. Gaynor JW, Ittenbach RF, Calafat AM, Burnham NB, Bradman A, Bellinger DC, Henretig FM, Wehrung EE, Ward JL, Russell WW, Spray TL. Perioperative Exposure to Suspect Neurotoxicants from Medical Devices in Newborns with Congenital Heart Defects. Ann Thorac Surg. 2019;107:567–572. [PubMed: 30071236]
18. Calafat AM, Needham LL, Silva MJ, Lambert G. Exposure to di-(2-ethylhexyl) phthalate among premature neonates in a neonatal intensive care unit. Pediatrics. 2004;113:e429–34. [PubMed: 15121985]
19. Demirel A, Çoban A, Yıldırım Ş, Doğan C, Sancı R, İnce Z. Hidden Toxicity in Neonatal Intensive Care Units: Phthalate Exposure in Very Low Birth Weight Infants. J Clin Res Pediatr Endocrinol. 2016;8:298–304. [PubMed: 27097850]
20. Su P-H, Chang Y-Z, Chang H-P, Wang S-L, Haung H-I, Huang P-C, Chen J-Y. Exposure to di(2-ethylhexyl) phthalate in premature neonates in a neonatal intensive care unit in Taiwan. Pediatr Crit Care Med. 2012;13:671–7. [PubMed: 22596068]
21. Huygh J, Clotman K, Malarvannan G, Covaci A, Schepens T, Verbrugghe W, Dirinck E, Van Gaal L, Jorens PG. Considerable exposure to the endocrine disrupting chemicals phthalates and bisphenol-A in intensive care unit (ICU) patients. Environ Int. 2015;81:64–72. [PubMed: 25955314]
22. Koch HM, Preuss R, Angerer J. Di(2-ethylhexyl)phthalate (DEHP): human metabolism and internal exposure-- an update and latest results. Int J Androl. 2006;29:155. [PubMed: 16466535]
23. Kessler W, Numtip W, Volkel W, Seckin E, Csanady GA, Putz C, Klein D, Fromme H, Filser JG. Kinetics of di(2-ethylhexyl) phthalate (DEHP) and mono(2-ethylhexyl) phthalate in blood and of DEHP metabolites in urine of male volunteers after single ingestion of ring-deuterated DEHP. Toxicol Appl Pharmacol. 2012;264:284–291. [PubMed: 22963843]
24. Casals-Casas C, Desvergne B. Endocrine disruptors: from endocrine to metabolic disruption. Annu Rev Physiol. 2011;73:135–162. [PubMed: 21054169]
25. Diamanti-Kandarakis E, Bourguignon JP, Giudice LC, Hauser R, Prins GS, Soto AM, Zoeller RT, Gore AC. Endocrine-disrupting chemicals: an Endocrine Society scientific statement. Endocr Rev. 2009;30:293–342. [PubMed: 19502515]
26. Halden RU. Plastics and health risks. Annu Rev Public Health. 2010;31:179–194. [PubMed: 20070188]
27. Swan SH. Prenatal phthalate exposure and anogenital distance in male infants. Environ Health Perspect. 2006;114:A88–9. [PubMed: 16451842]

28. Tickner JA, Schettler T, Guidotti T, McCally M, Rossi M. Health risks posed by use of Di-2-ethylhexyl phthalate (DEHP) in PVC medical devices: a critical review. Am J Ind Med. 2001;39:100–111. [PubMed: 11148020]
29. Trasande L, Sathyanarayana S, Spanier AJ, Trachtman H, Attina TM, Urbina EM. Urinary phthalates are associated with higher blood pressure in childhood. J Pediatr. 2013;163:747–53.e1. [PubMed: 23706605]
30. von Rettberg H, Hannman T, Subotic U, Brade J, Schaible T, Waag KL, Loff S. Use of di(2-ethylhexyl)phthalate-containing infusion systems increases the risk for cholestasis. Pediatrics. 2009;124:710–716. [PubMed: 19651587]
31. Kardas F, Bayram AK, Demirci E, Akin L, Ozmen S, Kendirci M, Canpolat M, Oztop DB, Narin F, Gumus H, Kumandas S, Per H. Increased Serum Phthalates (MEHP, DEHP) and Bisphenol A Concentrations in Children With Autism Spectrum Disorder. J Child Neurol. 2016;31:629–635. [PubMed: 26450281]
32. Green R, Hauser R, Calafat AM, Weuve J, Schettler T, Ringer S, Huttner K, Hu H. Use of di(2-ethylhexyl) phthalate-containing medical products and urinary levels of mono(2-ethylhexyl) phthalate in neonatal intensive care unit infants. Environ Health Perspect. 2005;113:1222–1225. [PubMed: 16140631]
33. Calafat AM, Weuve J, Ye X, Jia LT, Hu H, Ringer S, Huttner K, Hauser R. Exposure to bisphenol A and other phenols in neonatal intensive care unit premature infants. Environ Health Perspect. 2009;117:639–644. [PubMed: 19440505]
34. Sampson J, de Korte D. DEHP-plasticised PVC: relevance to blood services. Transfus Med. 2011;21:73–83. [PubMed: 21143327]
35. Barry YA, Labow RS, Rock G, Keon WJ. Cardiotoxic effects of the plasticizer metabolite, mono (2-ethylhexyl)phthalate (MEHP), on human myocardium. Blood. 1988;72:1438–1439.
36. Barry YA, Labow RS, Keon WJ, Tocchi M. Atropine inhibition of the cardiodepressive effect of mono(2-ethylhexyl)phthalate on human myocardium. Toxicol Appl Pharmacol. 1990;106:48–52. [PubMed: 2251683]
37. Jaimes R, Swiercz A, Sherman M, Muselimyan N, Marvar PJ, Posnack NG. Plastics and cardiovascular health: Phthalates may disrupt heart rate variability and cardiovascular reactivity. Am J Physiol - Hear Circ Physiol. 2017;313.
38. Labow RS, Barry YA, Tocchi M, Keon WJ. The effect of mono(2-ethylhexyl)phthalate on an isolated perfused rat heart-lung preparation. Environ Health Perspect. 1990;89:189–193. [PubMed: 2088746]
39. Rock G, Labow RS, Franklin C, Burnett R, Tocchi M. Hypotension and cardiac arrest in rats after infusion of mono(2-ethylhexyl) phthalate (MEHP), a contaminant of stored blood. N Engl J Med. 1987;316:1218–1219. [PubMed: 3574376]
40. Gillum N, Karabekian Z, Swift LM, Brown RP, Kay MW, Sarvazyan N. Clinically relevant concentrations of di (2-ethylhexyl) phthalate (DEHP) uncouple cardiac syncytium. Toxicol Appl Pharmacol. 2009;236:25–38. [PubMed: 19344669]
41. Posnack NG, Idrees R, Ding H, Jaimes Iii R, Stybayeva G, Karabekian Z, Laflamme MA, Sarvazyan N. Exposure to phthalates affects calcium handling and intercellular connectivity of human stem cell-derived cardiomyocytes. PLoS One. 2015;10:e0121927–e0121927. [PubMed: 25799571]
42. Sjoberg PO, Bondesson UG, Sedin EG, Gustafsson JP. Exposure of newborn infants to plasticizers. Plasma levels of di-(2-ethylhexyl) phthalate and mono-(2-ethylhexyl) phthalate during exchange transfusion. Transfusion. 1985;25:424–428. [PubMed: 4049487]
43. Rael LT, Bar-Or R, Ambruso DR, Mains CW, Slone DS, Craun ML, Bar-Or D. Phthalate esters used as plasticizers in packed red blood cell storage bags may lead to progressive toxin exposure and the release of pro-inflammatory cytokines. Oxid Med Cell Longev. 2009;2:166–71. [PubMed: 20592772]
44. Jaimes III R, Kuzmiak-Glancy S, Brooks DM, Kay MW. Short Term Functional Effects of Pyruvate Dehydrogenase Complex Activation in the Normoxic Heart. Am J Physiol Hear Circ Physiol. 2014;Under Revi.

45. Boukens BJ, Rivaud MR, Rentschler S, Coronel R. Misinterpretation of the mouse ECG: “musing the waves of Mus musculus”. J Physiol. 2014;592:4613–26. [PubMed: 25260630]
46. Erickson JR, Pereira L, Wang L, Han G, Ferguson A, Dao K, Copeland RJ, Despa F, Hart GW, Ripplinger CM, Bers DM. Diabetic hyperglycaemia activates CaMKII and arrhythmias by O-linked glycosylation. Nature. 2013;502:372–6. [PubMed: 24077098]
47. Perez-Alday EA, Li-Pershing Y, Bender A, Hamilton C, Thomas JA, Johnson K, Lee TL, Gonzales R, Li A, Newton K, Tereshchenko LG. Importance of the heart vector origin point definition for an ECG analysis: The Atherosclerosis Risk in Communities (ARIC) study. Comput Biol Med. 2019;104:127–138. [PubMed: 30472495]
48. Sedaghat G, Gardner RT, Kabir MM, Ghafoori E, Habecker BA, Tereshchenko LG. Correlation between the high-frequency content of the QRS on murine surface electrocardiogram and the sympathetic nerves density in left ventricle after myocardial infarction: Experimental study. J Electrocardiol. 2017;50:323–331. [PubMed: 28190561]
49. Rompelman O, Ros HH. Coherent averaging technique: a tutorial review. Part 1: Noise reduction and the equivalent filter. J Biomed Eng. 1986;8:24–9. [PubMed: 3951206]
50. Welch P The use of fast Fourier transform for the estimation of power spectra: A method based on time averaging over short, modified periodograms. IEEE Trans Audio Electroacoust. 1967;15:70–73.
51. Swift LM, Asfour H, Posnack NG, Arutunyan A, Kay MW, Sarvazyan N. Properties of blebbistatin for cardiac optical mapping and other imaging applications. Pflugers Arch Eur J Physiol. 2012;464:503–512. [PubMed: 22990759]
52. Kay M, Swift L, Martell B, Arutunyan A, Sarvazyan N. Locations of ectopic beats coincide with spatial gradients of NADH in a regional model of low-flow reperfusion. Am J Physiol Heart Circ Physiol. 2008;294:H2400–-5. [PubMed: 18310518]
53. Posnack NG, Jaimes R, Asfour H, Swift LM, Wengrowski AM, Sarvazyan N, Kay MW. Bisphenol A exposure and cardiac electrical conduction in excised rat hearts. Environ Health Perspect. 2014;122:384–90. [PubMed: 24487307]
54. Hondeghem LM, Carlsson L, Duker G. Instability and triangulation of the action potential predict serious proarrhythmia, but action potential duration prolongation is antiarrhythmic. Circulation. 2001;103:2004–13. [PubMed: 11306531]
55. Franz MR. The electrical restitution curve revisited: steep or flat slope--which is better? J Cardiovasc Electrophysiol. 2003;14:S140–7. [PubMed: 14760916]
56. Laughner JI, Ng FS, Sulkin MS, Arthur RM, Efimov IR. Processing and analysis of cardiac optical mapping data obtained with potentiometric dyes. Am J Physiol - Hear Circ Physiol. 2012;303.
57. Doshi AN, Walton RD, Krul SP, de Groot JR, Bernus O, Efimov IR, Boukens BJ, Coronel R. Feasibility of a semi-automated method for cardiac conduction velocity analysis of high-resolution activation maps. Comput Biol Med. 2015;65:177–183. [PubMed: 26045101]
58. Hunter JD. Matplotlib: A 2D Graphics Environment. Comput Sci Eng. 2007;9:90–95.
59. Mantegazza M, Franceschetti S, Avanzini G. Anemone toxin (ATX II)-induced increase in persistent sodium current: effects on the firing properties of rat neocortical pyramidal neurones. J Physiol. 1998;507 (Pt 1):105–16. [PubMed: 9490824]
60. O’Hara T, Virág L, Varró A, Rudy Y. Simulation of the Undiseased Human Cardiac Ventricular Action Potential: Model Formulation and Experimental Validation. PLoS Comput Biol. 2011;7:e1002061. [PubMed: 21637795]
61. Grandi E, Sobie EA, Clancy CE, Li Z, Colatsky T, Dutta S, Chang KC, Beattie KA, Sheng J, Tran PN, Wu WW, Wu M, Strauss DG. Optimization of an In silico Cardiac Cell Model for Proarrhythmia Risk Assessment. Front Physiol. 2017;8:616. [PubMed: 28878692]
62. Romero L, Cano J, Gomis-Tena J, Trenor B, Sanz F, Pastor M, Saiz J. In Silico QT and APD Prolongation Assay for Early Screening of Drug-Induced Proarrhythmic Risk. J Chem Inf Model. 2018;58:867–878. [PubMed: 29547274]
63. Tereshchenko LG, Josephson ME. Frequency content and characteristics of ventricular conduction. J Electrocardiol. 2015;48:933–937. [PubMed: 26364232]

64. Danik S, Cabo C, Chiello C, Kang S, Wit AL, Coromilas J. Correlation of repolarization of ventricular monophasic action potential with ECG in the murine heart. Am J Physiol Circ Physiol. 2002;283:H372–H381.

65. Qu Z, Xie Y, Garfinkel A, Weiss JN. T-wave alternans and arrhythmogenesis in cardiac diseases. Front Physiol. 2010;1:154. [PubMed: 21286254]

66. Hondeghem LM, Snyders DJ. Class III antiarrhythmic agents have a lot of potential but a long way to go. Reduced effectiveness and dangers of reverse use dependence. Circulation. 1990;81:686–90. [PubMed: 2153477]

67. Hondeghem LM. TRIad: foundation for proarrhythmia (triangulation, reverse use dependence and instability). Novartis Found Symp. 2005;266:235–44; discussion 244-50. [PubMed: 16050272]

68. Sirenko O, Cromwell EF, Crittenden C, Wignall JA, Wright FA, Rusyn I. Assessment of beating parameters in human induced pluripotent stem cells enables quantitative in vitro screening for cardiotoxicity. Toxicol Appl Pharmacol. 2013;273:500–507. [PubMed: 24095675]

69. Ben-Ari M, Schick R, Barad L, Novak A, Ben-Ari E, Lorber A, Itskovitz-Eldor J, Rosen MR, Weissman A, Binah O. From beat rate variability in induced pluripotent stem cell-derived pacemaker cells to heart rate variability in human subjects. Hear Rhythm. 2014;11:1808–1818.

70. Mandel Y, Weissman A, Schick R, Barad L, Novak A, Meiry G, Goldberg S, Lorber A, Rosen MR, Itskovitz-Eldor J, Binah O. Human embryonic and induced pluripotent stem cell-derived cardiomyocytes exhibit beat rate variability and power-law behavior. Circulation. 2012;125:883–893. [PubMed: 22261196]

71. Lakatta EG, Maltsev VA, Vinogradova TM. A coupled SYSTEM of intracellular Ca2+ clocks and surface membrane voltage clocks controls the timekeeping mechanism of the heart's pacemaker. Circ Res. 2010;106:659–673. [PubMed: 20203315]

72. Rubin RJ, Jaeger RJ. Some Pharmacologic and Toxicologic Effects of Di-2-Ethylhexyl Phthalate (DEHP) and Other Plasticizers. Environ Health Perspect. 1973;3:53–59. [PubMed: 4704572]

73. Aronson CE, Serlick ER, Preti G. Effects of di-2-ethylhexyl phthalate on the isolated perfused rat heart. Toxicol Appl Pharmacol. 1978;44:155–169. [PubMed: 675687]

74. Jalife J, Zipes DP. Cardiac electrophysiology. 2009;5th:1155.

75. Mariana M, Feiteiro J, Cairrao E. Cardiovascular Response of Rat Aorta to Di-(2-ethylhexyl) Phthalate (DEHP) Exposure. Cardiovasc Toxicol. 2017;88(pt 2):109–122.

76. Sheng J, Tran PN, Li Z, Dutta S, Chang K, Colatsky T, Wu WW. Characterization of loperamide-mediated block of hERG channels at physiological temperature and its proarrhythmia propensity. J Pharmacol Toxicol Methods. 2017;88:109–122. [PubMed: 28830713]

77. Kirchhof P, Engelen M, Franz MR, Ribbing M, Wasmer K, Breithardt G, Haverkamp W, Eckardt L. Electrophysiological effects of flecainide and sotalol in the human atrium during persistent atrial fibrillation. Basic Res Cardiol. 2005;100:112–121. [PubMed: 15696400]

78. Tereshchenko LG, Waks JW, Kabir M, Ghafoori E, Shvilkin A, Josephson ME. Analysis of speed, curvature, planarity and frequency characteristics of heart vector movement to evaluate the electrophysiological substrate associated with ventricular tachycardia. Comput Biol Med. 2015;65:150–160. [PubMed: 25842361]

What is known:

- Phthalate chemical exposure has been reported in patients undergoing invasive medical procedures that employ large quantities of plastic materials
- We previously reported that phthalate chemical exposure impairs cell coupling and slows conduction velocity in a cardiomyocyte cell model

What the study adds:

- Acute phthalate exposure slowed atrioventricular conduction and increased atrioventricular node effective refractory period in an intact, whole heart model
- Phthalate exposure prolonged action potential duration time, enhanced action potential triangulation and increased the ventricular effective refractory period
- Phthalate exposure slowed epicardial conduction velocity, which may be partly explained by inhibition of Nav1.5

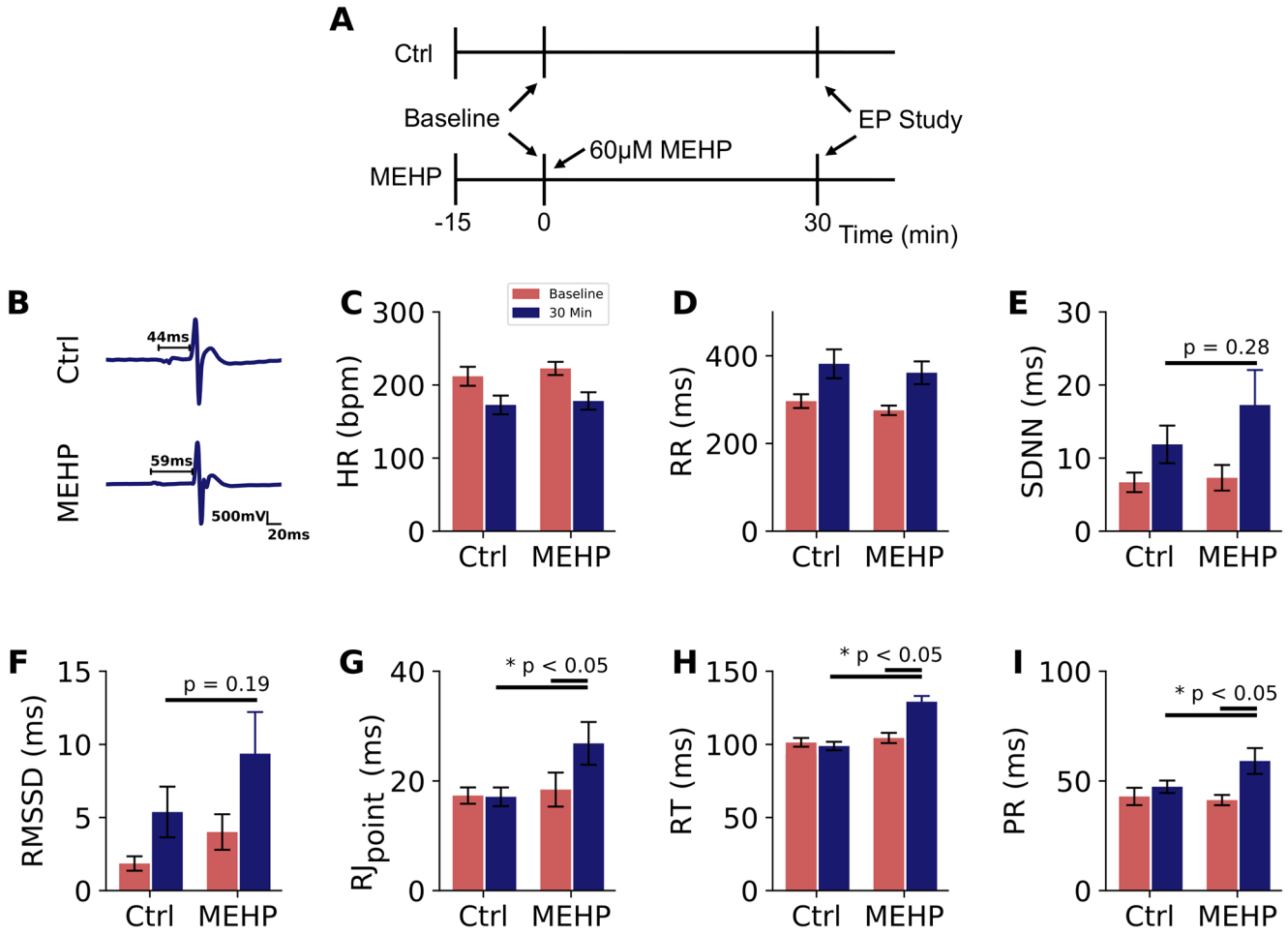

Figure 1.

Effect of MEHP on ECG characteristics during sinus rhythm. **(A)** Experimental protocol timeline; all ECG recordings were performed during sinus rhythm **(B)** ECG signals collected from excised, intact rat hearts with PR interval denoted. **(C)** Heart rate decreased with time of perfusion and following application of blebbistatin for mechanical uncoupling, with no difference between treatment groups. **(D)** Similar rate slowing was observed in the RR interval, and coincided with heart rate variability changes in **(E)** SDNN and **(F)** rMSSD after 30-min perfusion. **(G,H)** Prolonged depolarization and repolarization in MEHP-exposed hearts as measured from R to J inflection point (RJ_{point}) and R to T-wave (RT) **(G)** PR interval time was significantly lengthened in MEHP-exposed hearts compared to both baseline and control hearts after the same duration of perfusion ($p < 0.05$). Ctrl = control, EP = electrophysiology protocol, HR = heart rate, BPM = beats per minute, SDNN = standard deviation of the normal RR intervals, RMSSD = root means successive square difference. n ≥ 7 per group

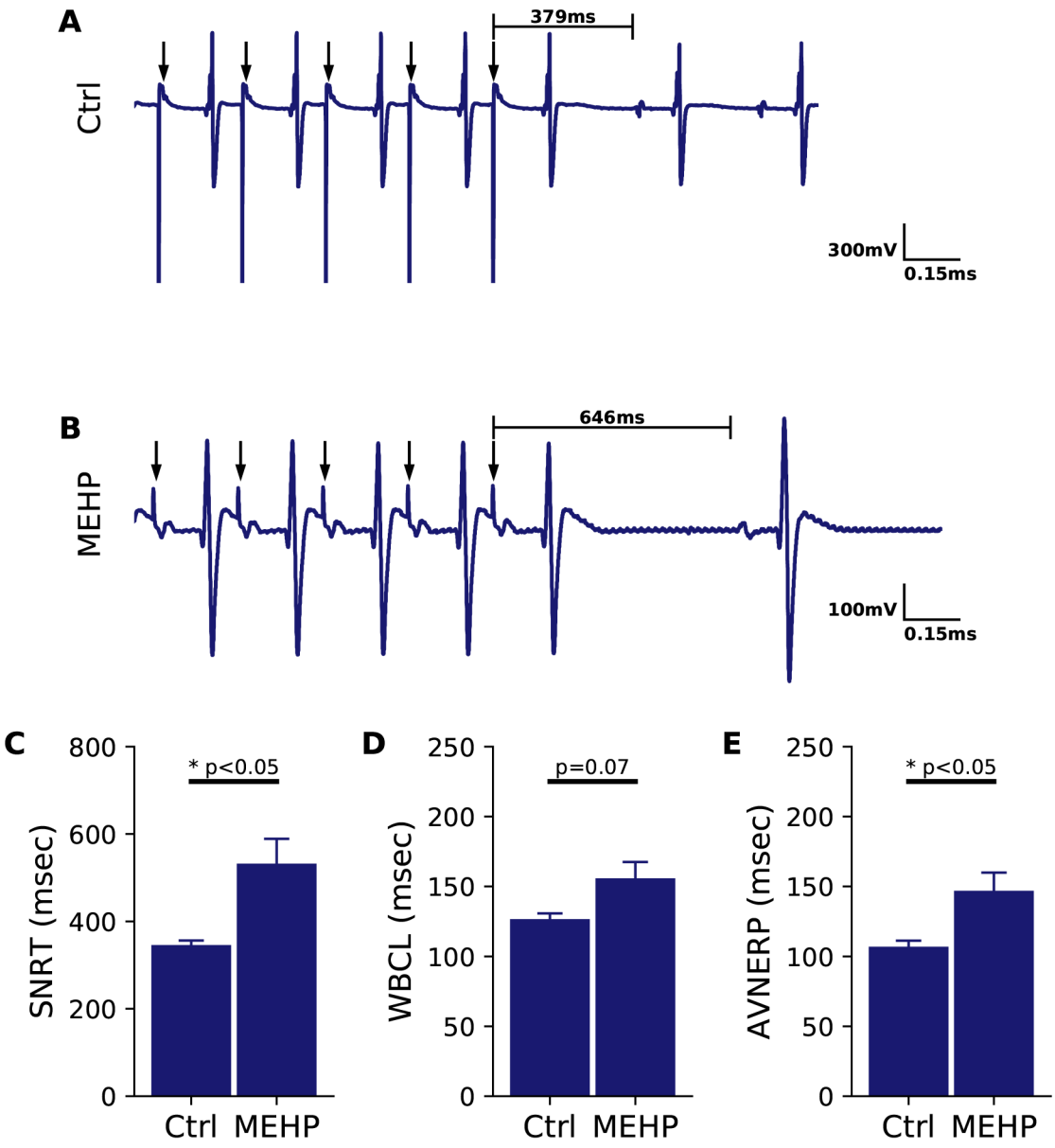

Figure 2.

Sinus node function and atrioventricular conduction altered after MEHP treatment. **(A)** ECG trace corresponding to a 200 ms PCL train (indicated by arrows) on the right atrium in a control heart. Sinus node recovery time (SNRT) is indicated as the delay between the cessation of pacing and the resumption of sinus node activity. **(B)** SNRT measured in MEHP-treated heart shows marked prolongation compared with control. **(C)** Aggregate SNRT analysis for MEHP-treated hearts and time-matched controls ($p < 0.05$). **(D)** Wenckebach cycle length (WBCL) measured as the earliest PCL in which Wenckebach phenomenon was visible ($p=0.07$). **(E)** Atrioventricular nodal refractory period (AVNERP) assessed by S1-S2 pacing on the right atrium was significantly lengthened in MEHP hearts compared with controls ($p < 0.05$). Ctrl = control, n=5-8 per group.

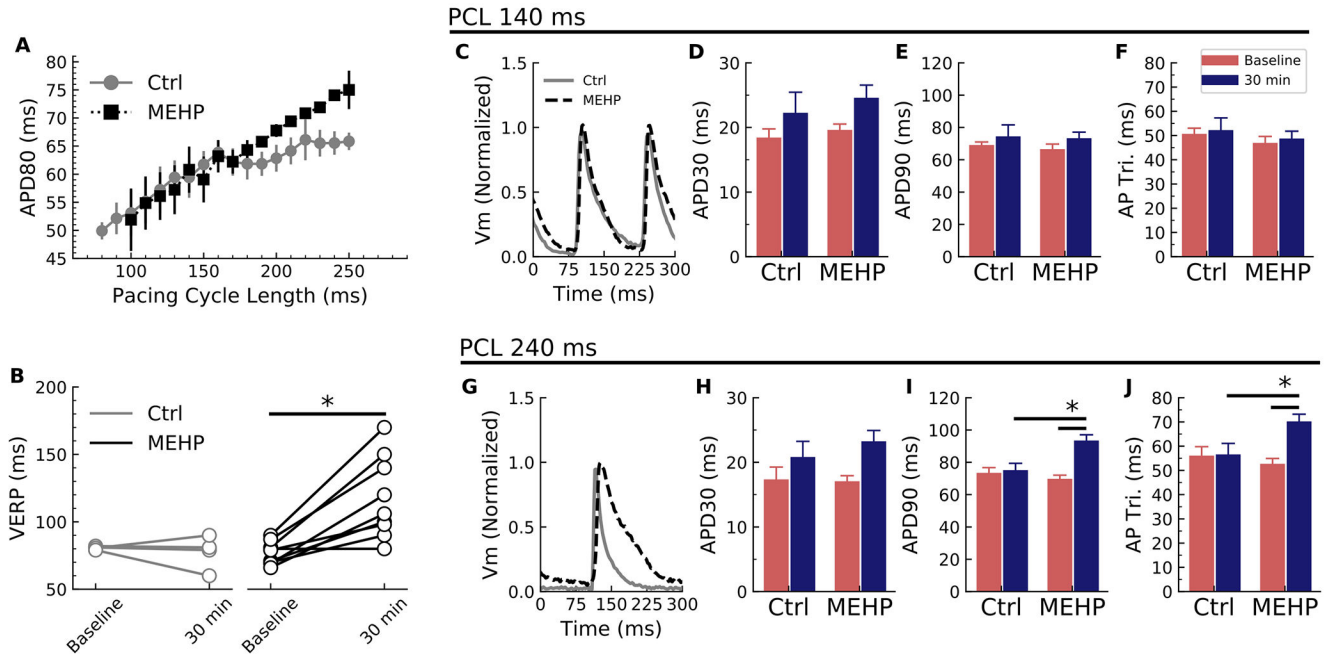

Figure 3.

MEHP causes action potential morphology changes with corresponding modification of the electrical restitution curve. **(A)** MEHP exposure caused the restitution curve to change from a biphasic form to a monophasic form with no plateau phase. The slope of the plateau on the control heart was 0.06 compared to 0.18 in the MEHP hearts. **(B)** Despite the similarities in the action potential duration at faster cycle lengths, the ventricular effective refractory period (VERP) was markedly prolonged in the MEHP-treated group ($p < 0.05$). **(C)** With rapid pacing (PCL=140 msec), the action potential duration appeared similar between the control and MEHP-treated groups: there were no difference between **(D)** APD30, **(E)** APD90 or **(F)** AP triangulation. **(G)** At slower cycle lengths (PCL=240 msec), the action potential morphology was quite different: while **(H)** APD30 was similar, **(I)** lengthening was apparent in the late phase as shown by APD90 ($p < 0.05$). **(J)** The effect on APD90 with no change on APD30 caused an increase in the triangulation shape of the AP after MEHP treatment ($p < 0.05$). Ctrl = control, Vm = transmembrane voltage, AP Tri = action potential triangulation. N=7 for each group.

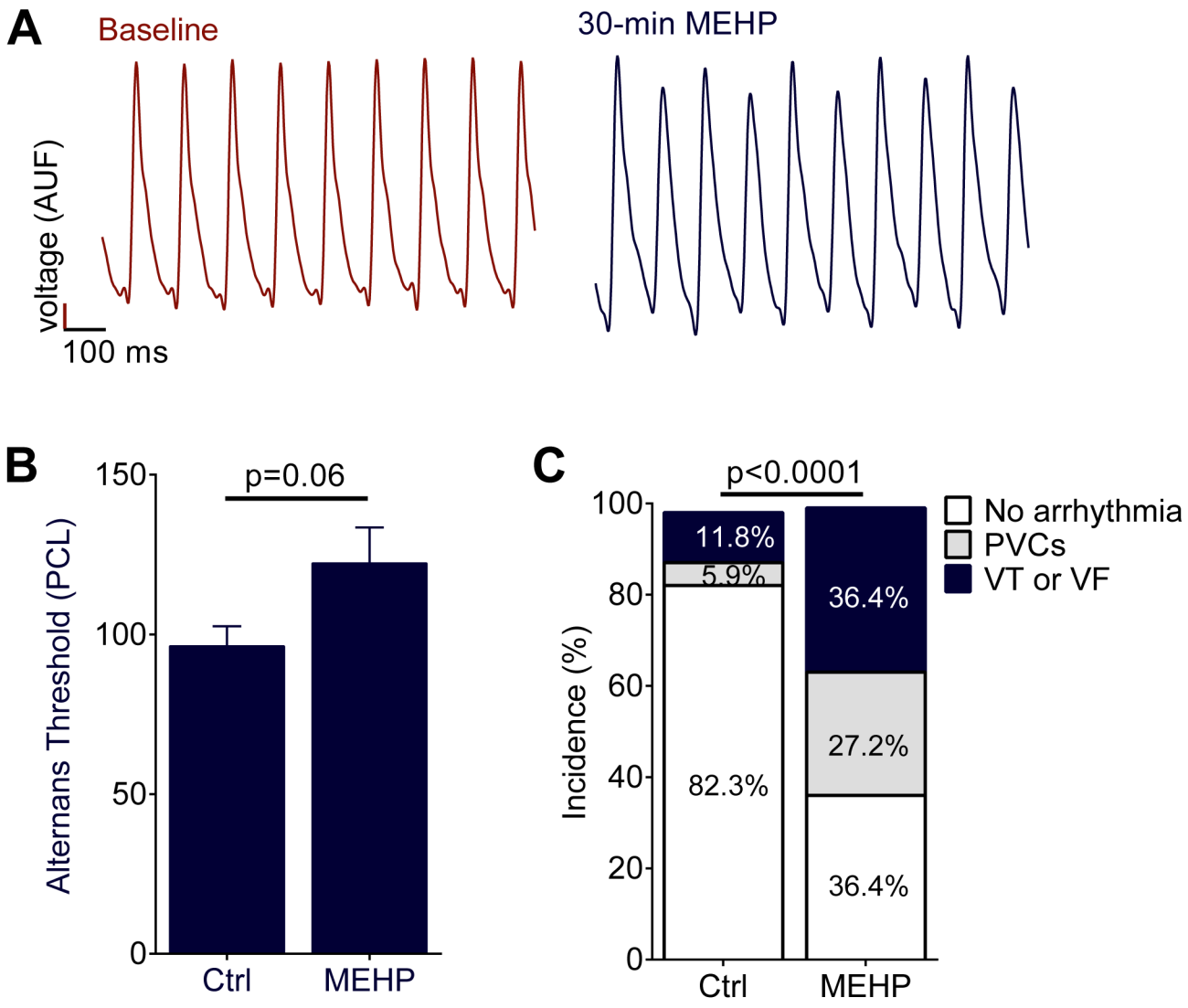

Figure 4.

Action potential alternans and arrhythmia susceptibility from MEHP exposure. **(A)** MEHP-treated hearts displayed an increased susceptibility to alternating action potential morphology at the same pacing cycle length compared to baseline as predicted by the change in electrical restitution (See Fig. 3A), PCL = 110msec this example. **(B)** The longest PCL which resulted in alternating action potentials (alternans threshold) was longer in the MEHP-treated hearts ($p = 0.06$). **(C)** Hearts after MEHP exposure became more susceptible to spontaneous arrhythmia as shown by a higher incidence of both PVCs and VT/VF following electrophysiological study ($p < 0.0001$, Chi-square test). AUF = arbitrary units of fluorescence, Ctrl = control. N=8 for each group.

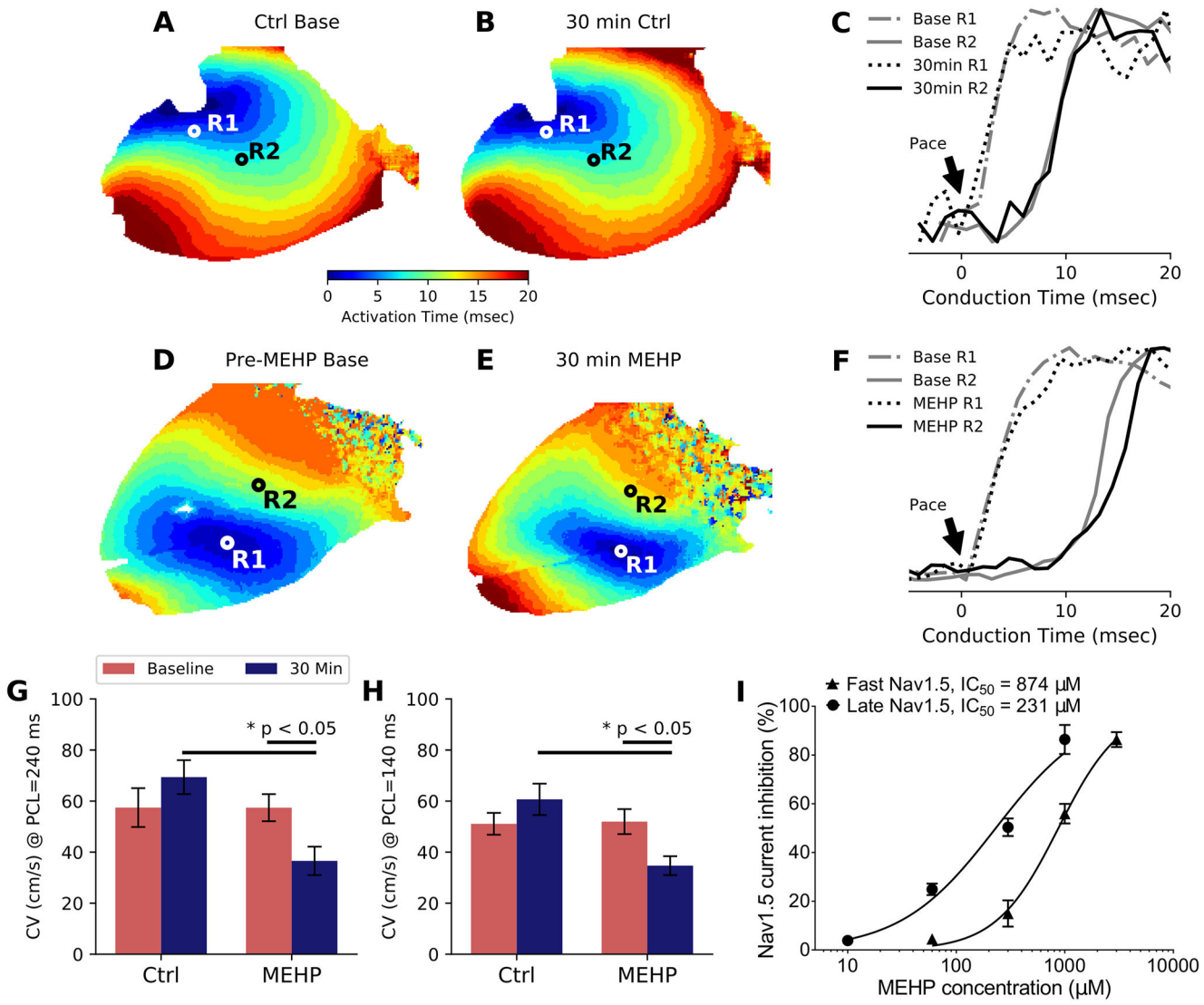

Figure 5.

Activation maps and measured conduction velocity after MEHP exposure. **(A)** Each pixel on the heart was assigned an activation time based on the maximum upstroke velocity in the fluorescent signal to create an isochrone map. Wavefronts are visible emanating from the center of the left ventricular epicardium where the cathodal pacing electrode was placed. **(B)** Following 30 minutes control-media perfusion, the activation maps did not show significant differences. **(C)** In control hearts, analysis of the pacing site (R1) and a distal site (R2) did not show significant differences in conduction time when compared between baseline and 30-min perfusion. **(D)** Pre-MEHP baseline showed similar conduction velocity as the control baseline. **(E)** After 30-min of MEHP exposure, the activation maps changed in morphology. **(F)** Analysis of the pacing site (R1) and distal site (R2) indicated a decreased upstroke velocity after 30-min of MEHP exposure. **(G)** Conduction velocity was significantly slower in MEHP-treated hearts compared to controls after 30 minutes at both PCL = 240 msec ($p < 0.05$) and **(H)** PCL = 140 msec ($p < 0.05$), with N=5 per group. **(I)** Sodium current (I_{Na}) was measured with HEK293 cells which stably express $Na_v1.5$. Fast sodium current (I_{Na}) was

measured in the absence of anemone toxin and half-maximal inhibition concentration (IC50) was determined at 874 μM. Late sodium current (I_{NaL}) was activated with anemone toxin and corresponding IC50 was determined at 231 μM (N=5 for each group). Ctrl = control, CV = conduction velocity

Table 1.

Measurements of clinical exposure to di-2-ethylhexyl phthalate (DEHP), and its metabolites including mono-2-ethylhexyl phthalate (MEHP).

Description	Concentration	Reference
Child, blood products (blood)	6.4 – 29 μg/ml DEHP (RBC unit) 27.6 – 405 μg/ml DEHP (plasma unit) 34.2 – 61.4 μg/ml DEHP (platelets)	Mallow, et al. 2014
Child, exchange transfusion (blood)	1.1 – 15.6 μg/ml MEHP 2.3 – 19.9 μg/ml DEHP	Sjoberg, et al. 1985
Child, blood products (blood)	3.0 – 15.6 μg/ml MEHP (blood unit) 36.8 – 84.9 μg/ml DEHP (blood unit)	Sjoberg, et al. 1985
Child, ECMO (blood)	26.8 μg/ml DEHP (14 days) 33.5 μg/ml DEHP (24 days)	Shneider, et al. 1989
Child, ECMO (blood)	10 – 30.8 μg/ml DEHP (circuit) 0 – 24.18 μg/ml DEHP (patient)	Karle, et al. 1997
Child, blood products (blood)	4.3 – 123 μg/ml DEHP (blood unit) 6 – 21.6 μg/ml DEHP (patient)	Plonait, et al. 1994
Child, intensive care unit (urine)	577 – 2357 μg/L MECPP 120 – 438 μg/L MEHHP 72 – 306 μg/L MEOHP 14.9 – 49.5 μg/L MEHP	Gaynor, et al. 2019
Child, intensive care unit (urine)	6.2 – 704 ng/ml MEHP (5–95th%) 290 – 13,161 ng/ml MEHHP (5–95th%) 243 – 10,413ng/ml MEOHP (5–95th%)	Calafat, et al. 2004
Child, intensive care unit (urine)	0 – 1234 ng/ml MEHP 0 – 5841 ng/ml MEOHP 0 – 5086 ng/ml MEHHP	Demirel, et al. 2016
Child, intensive care unit (urine)	0.049 – 1.273 μg/ml	Su, et al. 2012
Adult, blood products (blood)	1.1 – 18.7 μg/ml MEHP 72.5 – 295.2 μg/ml DEHP	Peck, et al. 1979
Adult, intensive care unit (blood)	0 – 171 μg/L MECPP 0 – 55.4 μg/L MEHHP 0 – 22.9 μg/L MEOHP	Huygh, et al. 2015
Adult, ECMO + CVVH (blood)	17.2 – 5194 μg/L MECPP 0 – 880 μg/L MEHHP 3.3 – 305 μg/L MEOHP	Huygh, et al. 2015
Adult, coronary bypass (blood)	15.4 – 72.9 mg/day DEHP 2.2 – 8 mg/kg MEHP	Barry, et al. 1989
Adult, heart transplantation (blood)	2.3 – 167.9 mg/day DEHP 0.25 – 18.8 mg/day MEHP	Barry, et al. 1989
Adult, hemodialysis (blood)	0.3 – 7.6 μg/ml DEHP 0.9 – 2.83 μg/ml MEHP	Pollack, et al. 1985
Adult, hemodialysis (blood)	2 – 3 μg/ml DEHP	Faouzi, et al. 1999

Abbreviations: ECMO, extracorporeal membrane oxygenation; CVVH, continuous venovenous hemofiltration; MEOHP, mono-2-ethyl-5-oxohexyl phthalate; MEHHP, mono-2-ethyl-5-hydroxyhexyl phthalate; MECPP, mono-2-ethyl-5-carboxypentyl phthalate. See references for details[7-21].